Bioorganic & Medicinal Chemistry Letters 21 (2011) 1852–1856

Contents lists available at ScienceDirect

Bioorganic & Medicinal Chemistry Letters

journal homepage: www.elsevier.com/locate/bmcl

Optimisation of ITK inhibitors through successive iterative design cycles

Matthias Herdemann [†], Alexander Weber [*,‡], Jérôme Jonveaux, Frank Schwoebel [§], Michael Stoeck, Isabelle Heit [*]

Nycomed GmbH, Byk-Gulden-Str. 2, D-78467 Konstanz, Germany

ARTICLE INFO

Article history:
Received 15 December 2010
Revised 9 January 2011
Accepted 10 January 2011
Available online 14 January 2011

Keywords:
Interleukin-2 inducible T cell kinase
Lead optimisation
In vivo testing
Anti-CD3 IL-2 mouse model

ABSTRACT

Based on a hit cluster of compounds inhibiting interleukin-2 inducible T-cell kinase (ITK) in the submicromolar range a series of ITK inhibitor libraries were synthesized. Through iterative design cycles including kinase crystal structure information, indolylindazole libraries were identified which showed low nanomolar activity in enzymatic and cellular assays. The potential of these novel lead series was confirmed through in vivo tests in an anti-CD3-IL2 mouse model. The intravenous administration of highly potent ITK inhibitor **11o** resulted in dose-dependent, efficient suppression of IL-2.

The non-receptor tyrosine kinase interleukin-2 inducible T cell kinase (ITK) is mainly expressed in T cells, mast cells and natural killer cells.[1] The protein kinase is activated in T cells through phosphorylation in the ITK activation loop by the kinase LCK after T-cell receptor (TCR) stimulation.[2] Phosphorylation of the ITK substrate PLC-γ1[3] leads to calcium mobilization, IL-2 production, proliferation and differentiation.[4] The lack of ITK results in reduced production of Th2 cytokines such as IL-4, IL-5 and IL-13.[5] ITK has been shown to play an important role in the development of T cell dependent late phase responses of allergic asthma. In studies with ITK$^{-/-}$ mice reduced lung inflammation including goblet cell hyperplasia, mucous production and airway hyper responsiveness were observed in an ovalbumin-induced allergic asthma model.[6] Similar results were reported with a selective ITK inhibitor[7] indicating the important role of ITK kinase activity in inflammatory processes. Therefore, the tyrosine kinase ITK is regarded as a promising therapeutic target for T cell mediated diseases.

Previously, we reported the identification of potent ITK inhibitors through focused library design wherein structural information provided by X-ray structures were included.[8] Docking studies of published ITK inhibitors **1** and **2** (Fig. 1) in ITK ATP binding pocket,[9] as well as in depth literature analysis led to an initial hit cluster represented by compound **3** (ITK IC_{50} = 5 μM).[8] Subsequent design cycles resulted in the identification of indolylpyrazolopyridine **4a** (ITK IC_{50} = 0.06 μM; CD4+T cells/IL-2 release IC_{50} = 1.4 μM) which was considered as a promising starting point for a lead finding project. Therefore, detailed docking studies were performed with

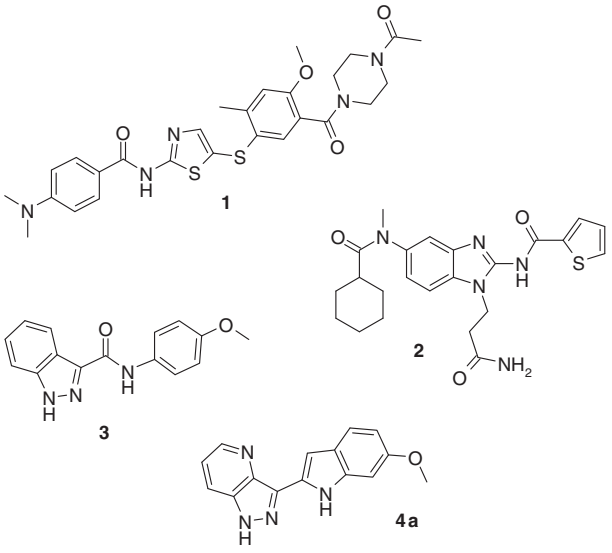

Figure 1. Published ITK inhibitors (**1**, **2**) and ITK inhibitors identified after the first (**3**) and second (**4a**) focused library design cycle. Indazole derivatives (**3**, ITK IC_{50} = 5 μM) were optimised through ring closure to indolylpyrazolopyridine derivatives (**4a**, ITK IC_{50} = 0.06 μM).

* Corresponding authors. Tel.: +49 7531 84 3130; fax: +49 7531 84 93130 (I.H.).
E-mail addresses: alexander.weber@boehringer-ingelheim.com (A. Weber), isabelle.heit@nycomed.com (I. Heit).
† Present address: EPO, Patentlaan 3-9, 2288 EE The Hague, Netherlands.
‡ Present address: Boehringer Ingelheim Pharma GmbH & Co. KG, 88400 Biberach, Germany.
§ Present address: NOXXON Pharma AG, Max-Dohrn-Str. 8-10, 10589 Berlin, Germany.

0960-894X/$ - see front matter © 2011 Elsevier Ltd. All rights reserved.
doi:10.1016/j.bmcl.2011.01.035

4a. Analysis of the docked conformation of **4a** within the protein environment indicated that substituents at position 6 of the indole moiety might improve the ITK binding affinity by addressing a small solvent exposed hydrophobic pocket (Ile-369, Leu-379, Phe-437, Fig. 2). Furthermore, substitutions at position 5 of the pyrazolopyridine ring system of **4a** could address polar amino acids in the sugar pocket or interact with Asp-500 of the DFG-motif. Prior to synthesis, chemical accessible modifications at position 6 of the indole motif as well as at position 5 of the pyrazolopyridine moiety of **4a** were virtually enumerated and docked in the ATP binding pocket of ITK.[10] Most interesting side chain variations were subsequently included in the optimisation cycles.

The first optimisation cycle was focused on the exploration of the indole's position 6, that is, on the replacement of the 6-methoxy group of compound **4a** (Fig. 2). The prepared compounds were first evaluated in an enzymatic assay using an ITK full-length enzyme. Subsequently, selected compounds were also tested for their inhibition of anti-CD3/anti-CD28 induced interleukin-2 (IL-2) release in primary human CD4+T cells. Protocols of both assays were identical with those reported previously.[8] The introduction of various groups resulted in the identification of several inhibitors having enzymatic and cellular potency similar to the potency of compound **4a**. However, these efforts did not result in a straightforward, significant increase of in vitro potency.[14]

Thus, further efforts focused on the indazole moiety, in particular on position 5. As discussed above, substitution at this position could allow additional interactions with the protein, in particular with polar amino acids in the sugar pocket or with Asp-500 of the DFG-motif.[9] The approach chosen for in depth investigation of position 5 is shown in Scheme 1. Starting from commercially available 5-nitro-indazole the Boc protected iodo-indazole **5** has been prepared by regioselective iodination under basic conditions followed by Boc protection in 77% yield. Key intermediates **7** have been obtained after Suzuki coupling of iodo-indazole **5** with commercially available indol-2-ylboronic acids **6** using a Pd(dppf) catalyst and cesium carbonate as a base, flash chromatography of the crude products with cyclohexane/ethyl acetate and subsequent

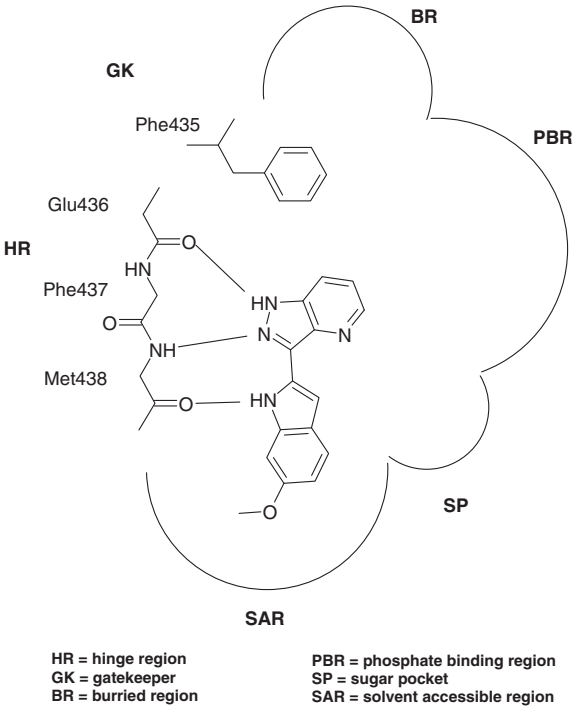

Figure 2. Proposed docked binding mode of indolylindazole derivatives **4a** in ITK identified after the second design cycle.[8]

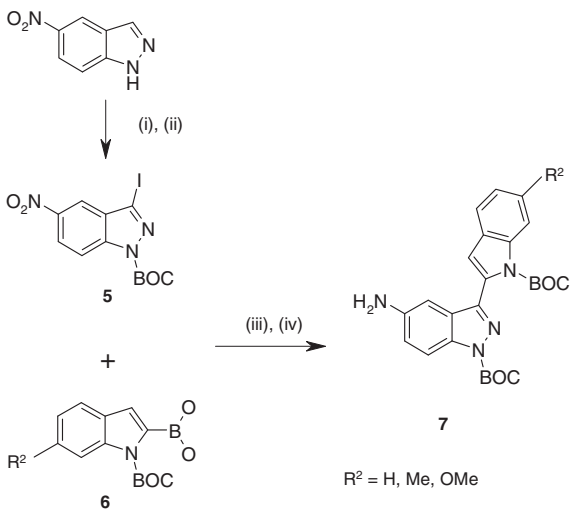

Scheme 1. Reagents and conditions: (i) I_2, KOH, DMF, 0 °C to rt, 2.5 h; (ii) Boc_2O, NEt_3, DMAP, DMF, 0 °C to rt, 1 h; (iii) $Pd(dppf)_2Cl_2$·DCM, Cs_2CO_3, dioxane, 80 °C, 2–4 h, argon; (iv) H_2, 10% Pd/C, AcOEt, rt, 15 h.

reduction of the nitro group to the amine group with hydrogen (1 bar) using Pd/C (10%) as catalyst. Yields for the sequence Suzuki coupling–hydrogenation were in the range of 62–77% (Scheme 1). The intermediate **7** has then been transformed into the amides **8**, sulfonamides **9**, urea compounds **10** and secondary amine derivatives **11** (Scheme 2). Reaction of **7** with acide chlorides in DME in the presence of triethylamine yielded quantitative conversion to the corresponding amides **8**. The crude product has then directly been deprotected with potassium carbonate in a mixture of water/methanol/THF to give the final compounds **8**. For the preparation of sulfonamides **9** best results were obtained with 1,6-lutidine as base in DCM, followed by the same deprotection procedure as applied for amides **8**. Treatment of **7** with isocyanates in DCM gave the desired urea function of compounds **10**. Standard conditions for reductive amination[11] of ketones and aldehydes with $NaBH(OAc)_3$ in DCM/AcOH were applied for the preparation of compounds **11**. The Boc protecting group at the secondary amines being stable under the above mentioned deprotection conditions secondary amines such as **11h**, **11m** and **11o**[12] have been isolated after deprotection with TFA in DCM. Intermediates **7** have also been deprotected directly to give the corresponding amino compounds **12** (Scheme 2). The synthetic approach which was applied for amides **8** which were substituted at position 5 of the indazole has also been used for the preparation of amides **13** which were substituted at position 6 of the indazole (Table 1). These amides **13** were thus prepared using commercially available 6-nitro-indazole as starting material instead of 5-nitro-indazole (Scheme 1) which were applied for amides **8** (Scheme 2).

The amide series **8** have been evaluated while varying at the same time the substituent R^2 at position 6 of the indole moiety. Acetylamide **8a** exhibited an enzymatic IC_{50} value of 67 nM (Table 1). This amounts to an about twofold activity increase compared to 170 nM for the corresponding amino compound **12** wherein R^2 represents also a methyl group (Scheme 2). As shown in Table 1 small substituents are well tolerated (**8b** and **8c**), larger substituents such as a cyclohexyl moiety or a phenyl ring resulted in a dramatic decrease of the enzymatic potency (**8d** and **8f**). However, compounds having a heteroatom in the *para*-position of the ring, such as the oxygen of tetrahydropyran (**8e**) or the cyano substituent (**8g**) performed better than the corresponding compounds **8d** and **8f**. In general, the measured enzymatic potency of compounds which were not substituted at position 6

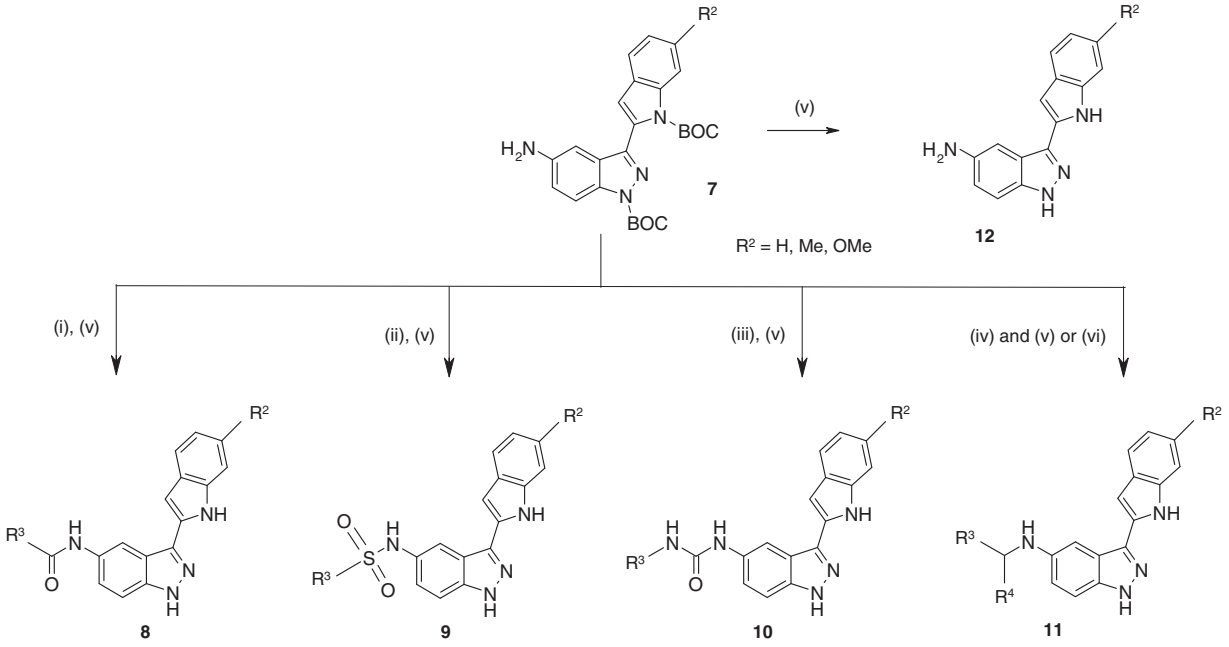

Scheme 2. Reagents and conditions: (i) R^3COCl, NEt_3, DME, 0 °C to rt, 15 h; (ii) R^3SO_2Cl, 2,6-lutidine, DCM, 0 °C to rt, 15 h; (iii) R^3NCO, DCM, 0 °C to rt, 15 h; (iv) R^3R^4CO, $NaBH(OAc)_3$, AcOH, DCM, rt, 18 h; (v) 4 M K_2CO_3aq, MeOH, THF, 60 °C, 3–4 h; (vi) TFA, DCM, 0 °C to rt, 4 h.

Table 1
Amide substituents at positions 5 (**8**) and 6 (**13**) of the indazole

Compd	R^2	R^3	IC_{50} enzyme[a] (μM)	IC_{50} cell, IL-2[a] (μM)
8a	Me	Me	0.067	1.0
8b	Me	Methoxy-methyl	0.12	—
8c	Me	Dimethylamino-methyl	0.065	0.6
8d	Me	Cyclohexyl	0.99	—
8e	Me	Tetrahydro-2*H*-pyran-4-yl	0.26	—
8f	Me	Phenyl	2.30	—
8g	Me	4-Cyano-phenyl	0.83	—
8h	Me	Furan-2-yl	0.53	—
8i	H	Me	0.14	—
8k	H	Methoxy-methyl	0.16	—
8l	H	Cyclohexyl	1.60	—
8m	H	Phenyl	1.50	—
8n	MeO	Me	0.087	—
8o	MeO	Methoxy-methyl	0.098	0.5
8p	MeO	Cyclohexyl	0.90	—
8q	MeO	Phenyl	1.00	—
13a	Me	Me	0.22	—
13b	Me	Methoxy-methyl	0.34	—
13c	Me	Cyclohexyl	>50	—
13d	Me	Phenyl	>50	—

[a] Means from 2 to 3 independent experiments.

Table 2
Sulfonamide and urea derivatives obtained through substitution at position 5 of the indazole

Compd	R^2	R^3	IC_{50} enzyme[a] (μM)	IC_{50} cell, IL-2[a] (μM)
9a	Me	Me	0.036	0.4
9b	Me	Phenyl	0.069	0.4
9c	Me	2-Fluoro-phenyl	0.047	1.0
9d	Me	3-Fluoro-phenyl	0.045	0.8
9e	Me	4-Fluoro-phenyl	0.25	2.9
9f	Me	3-Methoxy-phenyl	0.046	0.9
9g	Me	4-Methoxy-phenyl	1.41	0.7
9h	Me	3,5-Dimethyl-isoxazol-4-yl	0.13	0.5
9i	Me	1-Methyl-1*H*-imidazol-4-yl	0.026	0.4
9k	Me	1,2-Dimethyl-1*H*-imidazol-4-yl	0.043	0.9
9l	Me	1,3,5-Trimethyl-1*H*-pyrazol-4-yl	0.085	1.0
9m	Me	2,4-Dimethyl-thiazol-5-yl	0.19	2.0
10a	Me	Ethyl	0.083	0.6
10b	Me	Cyclohexyl	0.78	3.2
10c	Me	Phenyl	0.73	—
10d	Me	3,5-Dimethyl-isoxazol-4-yl	0.072	0.3
10e	Me	Benzyl	0.75	—
10f	Me	Furan-2-yl-methyl	0.31	—

[a] Means from 2 to 3 independent experiments.

of the indole moiety (such as **8i**–**8m**) was slightly reduced compared to that of derivatives wherein R^2 was either a methyl group or a methoxy group (**8n**–**8q**). As predicted by docking studies, small substituents were tolerated at position 6 of the indazole (**13a** and **13b**), but compounds having larger substituents (**13c** and **13d**) were inactive (Table 1).

In view of the results obtained for R^2 = H, Me and OMe within the amide series, further series were prepared and tested exclusively with the Me substituent. The change from the amide function to a sulfonamide resulted in a significant activity increase of both enzymatic and cellular potency (Table 2). Methylsulfonamide **9a** had an IC_{50} of 36 nM in the enzymatic assay and 0.4 μM in the cellular assay. Due to the different molecular geometry of sulfonamides compared to that of amides also larger residues such as substituted phenyl groups are tolerated (**9b**–**9d** and **9f**), except *para*-substituted phenyl groups (**9e** and **9g**). Interestingly, both imidazole derivatives **9i** and **9k** showed promising enzymatic potency. The cellular potency observed for **9i** was identical to that of **9a** (0.4 μM). The activities within the urea series **10** were similar to those measured for the amides **8** (Table 2). Small substituents such as an ethyl group (**10a**) resulted in a slight increase of enzymatic potency. Larger residues such as cyclohexyl and phenyl led to a significant loss of potency (**10b**–**10c** and **10e**–**10f**). Both the enzymatic and cellular potency of **10d** were significantly increased compared to **10c**.

With respect to the variations introduced through reductive amination at position 5 of the indazole ring, the attachment of linear or cyclic aliphatic residues reduced the potency (Table 3 **11a**–**11g**) compared to 170 nM for the corresponding amino compound **12** wherein R^2 represents also a methyl group. However, the

Table 3
Amine substituents at the position 5 of the indazole

Compd	R^2	CHR^3R^4	IC_{50} enzyme[a] (μM)	IC_{50} cell, IL-2[a] (μM)
11a	Me	Isopropyl	0.72	–
11b	Me	Isobutyl	0.86	–
11c	Me	Cyclobutyl	0.62	–
11d	Me	Cyclohexyl	1.20	–
11e	Me	4-Phenyl-cyclohexyl	12.0	–
11f	Me	Cyclohexyl-methyl	1.70	–
11g	Me	Benzyl	0.53	–
11h	Me	Piperidin-4-yl	0.016	0.09
11i	Me	*N*-Methyl-piperidin-4-yl	0.010	0.12
11k	Me	*N*-Benzyl-piperidin-4-yl	0.023	0.50
11l	Me	*N*-Acetyl-piperidin-4-yl	0.37	–
11m	Me	Piperidin-3-yl	0.077	–
11n	Me	*N*-Ethyl-piperidin-3-yl	0.066	–
11o	Me	Pyrrolidin-3-yl	0.08	0.02
11p	Me	*N*-Benzyl-pyrrolidin-3-yl	0.03	0.35
11q	Me	1-Dimethylamino-propan-2-yl	0.027	–

[a] Means from 2 to 3 independent experiments.

bioisosteric replacement of one CH_2 of the cyclohexyl ring of **11d** by a nitrogen resulted in highly potent compounds. While **11d** showed an IC_{50} of 1.2 μM, **11h** inhibited ITK in the enzymatic assay with an IC_{50} of 16 nM and was also highly potent in the cellular assay (90 nM). This dramatic activity increase has been observed for a whole series of basic heterocycles (**11h–11k** and **11m–11p**). In contrast, N-acetylated compound **11l** was far less active than the basic analogues. No significant difference in enzymatic potency was observed for either the secondary amine **11h** or the tertiary amines **11i** and **11k**. The change from the 4-piperidyl ring to a 3-piperidyl ring led to a decrease of the enzymatic potency. **11m** inhibited ITK with an IC_{50} of 77 nM, tertiary amine **11n** with an IC_{50} of 66 nM. The enzymatic potencies observed for the five-membered pyrrolidin compounds **11o** (IC_{50} = 11 nM) and **11p** (IC_{50} = 30 nM) were in the same range as for the 4-piperidyl inhibitors. Moreover, with an IC_{50} of 20 nM in the cellular assay secondary amine **11o** was the most potent indolylindazole ITK inhibitor (Table 3). Ring opening of the pyrrolidine heterocycle resulted in a minor decrease of the enzymatic ITK inhibition (**11q**). The significantly increased binding affinity to the ITK enzyme could be understood in the light of performed docking studies. Figure 3 shows the binding mode of **11o** within the ITK ATP binding pocket. Main hydrogen-bond interactions were made with backbone carbonyl oxygen of Glu-436 and backbone nitrogen and oxygen of Met-438 in the hinge region. The affinity increase of **11o** and related basic compounds compared to parent compound **4a** could be explained with the additional interaction made with Asp-500 (Fig. 3). Unfortunately, crystal structures of **11o** or its analogues with the target protein could not be observed. However, the proposed binding mode was in line with the obtained SAR information for this lead series.

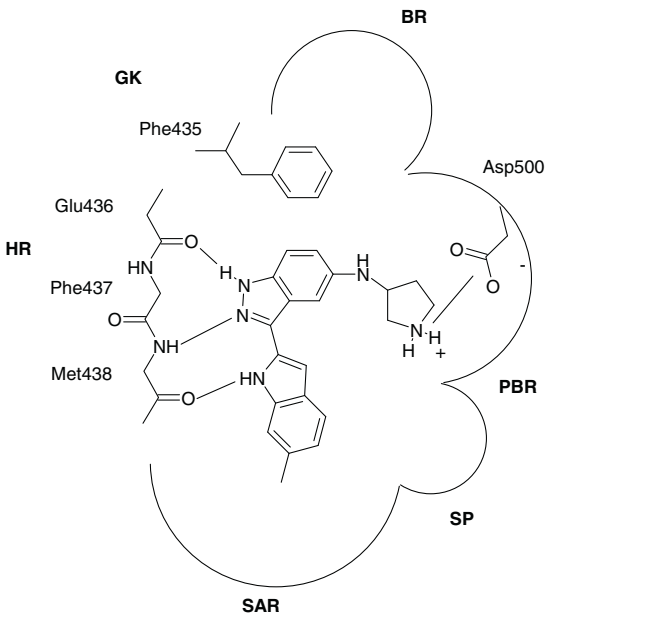

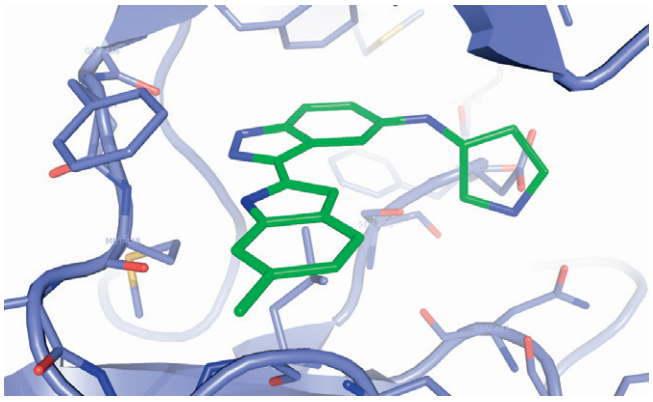

Figure 3. Proposed docked binding mode of **11o** in ITK ATP binding pocket.

Previous selectivity profiling of compound **4a** in a panel of about 30 kinases revealed equipotency against the receptor tyrosine kinase Flt3.[8] Therefore, four representative inhibitors were selected for profiling in a large panel of 108 kinases.[14] Sulfonamide **9k** (Scheme 2 and Table 2) and the amines **11k** and **11o** (Scheme 2 and Table 3) were tested at two different concentrations (0.1 and 1.0 micromolar). The same screening was also performed with an alkoxy derivative of **4a** wherein the OCH_3 substituent was replaced by a bulkier OCH_2–benzoyl residue at the indole's position 6. The tests revealed that sulfonamide **9k** and the alkoxy derivative of **4a** exhibited the best selectivity since only 10 further kinases out of 108 were inhibited by both compounds at 0.1 micromolar concentration to a similar extend as ITK. Basic compounds **11k** and **11o** showed a medium selectivity inhibiting about 20 further kinases in a similar range as ITK. All compounds inhibited Aurora A, Flt3, JAK2, Ret and TrkA equipotently with regard to ITK. Even though especially compound **9k** showed a nicely improved profile,

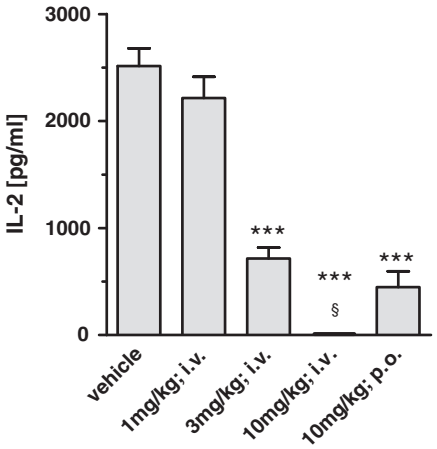

Figure 4. Level of IL-2 release 2 h after anti-CD3 antibody stimulation after pretreatment with compound **11o**. Data are mean ± SEM, $n = 8$ mice per group. $^{***}p \leqslant 0.001$ (compared to vehicle; ANOVA followed by Dunnett's test; § = below detection limit).

the goal of an excellent selectivity profile has not yet been achieved in this optimisation process.

After further in vitro profiling, compound **11o** was selected for in vivo evaluation in an anti-CD3 antibody-induced IL-2 mouse model.[13] The choice for **11o** was made based on its excellent in vitro potency of 11 nM in the enzymatic and 20 nM in the cellular assay, combined with acceptable cytotoxicity and favourable physicochemical properties such as solubility and low plasma protein binding (data not shown). Intravenous single administration of **11o** resulted in dose-dependent IL-2 suppression (Fig. 4). An intravenous dose of 10 mg/kg resulted in IL-2 concentration levels below the detection limit. The ED_{50} of IL-2 inhibition was calculated to be 2.1 mg/kg. Moreover, after po administration of 10 mg/kg of **11o** the measured IL-2 inhibition was >80% compared to the vehicle. Intravenous, as well as oral treatment with **11o** was well tolerated at all dose levels and no obvious side effects were observed compared to the positive control group.

In conclusion, highly potent compounds have been identified after optimisation within a novel class of ITK inhibitors. Lead compound **11o** has enzymatic and cellular activities in the low nanomolar range. Dose-dependent, efficient suppression of anti-CD3 antibody induced IL-2 release was observed in an in vivo mouse model after intravenous administration. Furthermore, in the same animal model, oral administration of 10 mg/kg of **11o** resulted in potent inhibition of IL-2 secretion which indicated good oral bioavailability of the compound that was also well tolerated.

Acknowledgements

We thank J. Wilsberg for skillful synthetic support, M. Beschle and K.-M. Nagy for LC–MS purifications, Dr. H.-C. Holst and Mr. T. Kottysch for NMR analyses, G. Prehn, E. Rolser, G. Schaffrath, J. Schindler and Dr. T. Ciossek for biological in vitro testing, J. Wegmann, A. Hirrle and A. Haschke for the testing in vivo. We gratefully thank Professor Dr. G. Baier (University of Innsbruck) for scientific advice.

Supplementary data

Supplementary data associated with this article can be found, in the online version, at doi:10.1016/j.bmcl.2011.01.035.

References and notes

1. (a) Yamada, N.; Kawakami, Y.; Kimura, H.; Fukamachi, H.; Baier, G.; Altman, A.; Kato, T.; Inagaki, Y.; Kawakami, T. *Biochem. Biophys. Res. Commun.* **1993**, *192*, 231; (b) Siliciano, J. D.; Morrow, T. A.; Desiderio, S. V. *Proc. Natl. Acad. Sci. U.S.A.* **1992**, *89*, 11194.
2. Heyeck, S. D.; Wilcox, H. M.; Bunnell, S. C.; Berg, L. J. *J. Biol. Chem.* **1997**, *272*, 25401.
3. Liu, K. Q.; Bunnell, S. C.; Gurniak, C. B.; Berg, L. J. *J. Exp. Med.* **1998**, *187*, 1721.
4. (a) Schaeffer, E. M.; Debnath, J.; Yap, G.; McVicar, D.; Liao, X. C.; Littman, D. R.; Sher, A.; Varmus, H. E.; Lenardo, M. J.; Schwartzberg, P. L. *Science* **1999**, *284*, 638; (b) Fowell, D. J.; Shinkai, K.; Liao, X. C.; Beebe, A. M.; Coffman, R. L.; Littman, D. R.; Locksley, R. M. *Immunity* **1999**, *11*, 399.
5. Miller, A. T.; Wilcox, H. M.; Lai, Z.; Berg, L. J. *Immunity* **2004**, *21*, 67.
6. Mueller, C.; August, A. *J. Immunol.* **2003**, *170*, 5056.
7. Lin, T. A.; McIntyre, K. W.; Das, J.; Liu, C.; O'Day, K. D.; Penhallow, B.; Hung, C. Y.; Whitney, G. S.; Shuster, D. J.; Yang, X.; Townsend, R.; Postelnek, J.; Spergel, S. H.; Lin, J.; Moquin, R. V.; Furch, J. A.; Kamath, A. V.; Zhang, H.; Marathe, P. H.; Perez-Villar, J. J.; Doweyko, A.; Killar, L.; Dodd, J. H.; Barrish, J. C.; Wityak, J.; Kanner, S. B. *Biochemistry* **2004**, *43*, 11056.
8. Herdemann, M.; Heit, I.; Bosch, F.-U.; Quintini, G.; Scheipers, C.; Weber, A. *Bioorg. Med. Chem. Lett.* **2010**, *20*, 6998.
9. Brown, K.; Long, J. M.; Vial, S. C.; Dedi, N.; Dunster, N. J.; Renwick, S. B.; Tanner, A. J.; Frantz, J. D.; Fleming, M. A.; Cheetham, G. M. *J. Biol. Chem.* **2004**, *279*, 18727.
10. (a) Gerber, P. R.; Muller, K. M. A. B. *J. Comput. Aided Mol. Des.* **1995**, *9*, 251; (b) www.moloc.ch.
11. (a) Abdel-Magid, A. F.; Maryanoff, C. A.; Carson, K. G. *Tetrahedron Lett.* **1990**, *31*, 5595; (b) Abdel-Magid, A. F.; Maryanoff, C. A. *Synlett* **1990**, *111*, 537.
12. *Preparation of* **11o** *for in vivo testing*: Intermediate **7** (R^2 = Me; 2.80 mmol) was dissolved in DCM (25 mL). Acetic acid (0.48 mL) and then 1-Boc-pyrrolidin-3-one (4.20 mmol) were added. After stirring over 30 min at rt $NaBH(OAc)_3$ was added and the reaction mixture was stirred overnight. After addition of H_2O (20 mL) and saturated $NaHCO_{3aq}$ (5 mL) the organic and aqueous layers were separated, the aqueous layer was extracted with DCM (2 × 20 mL). The combined organic phases were dried over $MgSO_4$ and the solvent was removed under reduced pressure. The residue was dissolved in DCM (15 mL). At 0 °C TFA (10 mL) was added, the ice bath was removed and the mixture was stirred for 4 h. The reaction mixture was then concentrated under reduced pressure. Remaining TFA was removed by addition of toluene (5 mL) and followed by concentration. Subsequently, DCM (40 mL) and saturated $NaHCO_{3aq}$ (40 mL) were added. After separation of the organic and aqueous layers the aqueous layer (pH 10) was extracted with DCM (2 × 40 mL) and the combined organic phases were dried over $MgSO_4$. Removal of the solvent under reduced pressure gave the desired crude product. Purification of **11o** was performed by flash chromatgraphy. After a first chromatography on basic silica gel with DCM/MeOH (95:5) the product (purity 90%) was submitted to a second flash chromatography with cyclohexane/AcOEt/MeOH (60:20:20) as eluent to provide 216 mg (23% overall yield) of pure **11o**.
13. *Anti-CD3 IL-2 mouse model*: Female BALB/c mice (~20 g body weight) received either one of the three doses of **11o** (1, 3, 10 mg/kg body weight) intravenously 10 min or orally (10 mg/kg) 1 h before intravenous injection of a monoclonal anti-CD3 stimulating antibody (10 μg/kg body weight, BD PharMingen, clone: 145-2C11, Cat. No.01080D). The positive control group received vehicle (saline) intravenously and the antibody at the same dose for an equivalent length of time. Two hours after stimulation mice were finally anaesthetized and blood samples were taken by heart puncture. Suppression of antibody induced stimulation was described by the determination of IL-2 levels in plasma samples. Cytokine concentrations were measured by ELISA (R&D Systems, Quantikine mouse IL-2 ELISA Kit, Cat. No. M2000).
14. Supplementary data.